Hindawi Publishing Corporation
International Journal of Polymer Science
Volume 2013, Article ID 323854, 14 pages
http://dx.doi.org/10.1155/2013/323854

*Research Article*

# Effects of the Addition of *Ortho*- and *Para*-$NH_2$ Substituted Tetraphenylporphyrins on the Structure of Nylon 66

**Luis A. Díaz-Alejo,[1] E. Carmina Menchaca-Campos,[2] J. Uruchurtu Chavarín,[2] R. Sosa-Fonseca,[3] and Miguel A. García-Sánchez[1]**

[1] *Departamento de Química, Universidad Autónoma Metropolitana-Iztapalapa, San Rafael Atlixco 186, Colonia Vicentina, 09340 Mexico City, DF, Mexico*
[2] *Centro de Investigación en Ingeniería y Ciencias Aplicadas (CIICAp), Universidad Autónoma del Estado de Morelos (UAEM), Avenida Universidad 1001, Colonia Chamilpa, 62209 Cuernavaca, MOR, Mexico*
[3] *Departamento de Física, Universidad Autónoma Metropolitana-Iztapalapa, San Rafael Atlixco 186, Colonia Vicentina, 09340 Mexico City, DF, Mexico*

Correspondence should be addressed to Miguel A. García-Sánchez; mags@xanum.uam.mx

Received 30 March 2013; Revised 27 June 2013; Accepted 16 July 2013

Academic Editor: Enrique Vigueras Santiago

Copyright © 2013 Luis A. Díaz-Alejo et al. This is an open access article distributed under the Creative Commons Attribution License, which permits unrestricted use, distribution, and reproduction in any medium, provided the original work is properly cited.

The synthetic tetrapyrrole macrocycles, such as porphyrins ($H_2P$) and phthalocyanines ($H_2Pc$), exhibit interesting physicochemical properties suitable to be used in modern technology. For many applications, those species should be trapped or fixed inside graphite, hydrotalcites, silica, $TiO_2$, or polymers. Methodologies for the optimization of the properties of porphyrins, trapped or fixed inside polymers, have been barely developed. Our research works in the development of methodologies for the optimization of incorporation and display of properties of tetrapyrrole macrocycles inside inorganic, polymeric, or hybrid networks. This paper shows some results about the effect of the spatial disposition of the amine ($-NH_2$) groups attached on the periphery of substituted tetraphenylporphyrins, on the Nylon 66 structure and on the display of the physicochemical properties of the trapped macrocycles. Nylon 66 was synthesized from adipoyl chloride and hexamethylenediamine in presence of tetraphenylporphyrins substituted with $-NH_2$ groups localized at the *ortho- or para*-positions of the phenyls. Cobalt complexes formation was used to quantify the amount of porphyrins in the polymer fibers. Characterization results show that the spatial position of amine groups of the porphyrins has important structural and textural effect on the Nylon 66 fibers and on the fluorescence of the porphyrins integrated into the fibers.

## 1. Introduction

Porphyrins are tetrapyrrole macrocyclic compounds playing a transcendental role in nature as one of the principal components of molecules such as (i) chlorophyll, (ii) the *heme* group in blood and cytochromes and (iii) cyanocobalamin (Vitamin $B_{12}$) [1–3]. Formally, porphyrins are modified or substituted aromatic tetrapyrrole macrocyclic compounds derived from porphin (Figure 1), which consists of four pyrrole rings bonded through *methine* (=CH) bridges in order to form a planar and highly conjugated macrocycle. In the free bases of porphyrins, the two *pyrrolic* hydrogens can be substituted by a cation, and the remaining two nitrogens tend to easily coordinate with a metal nucleus as to form a stable metalloporphyrin. Synthetic porphyrinic complexes, involving practically all metallic elements of the periodic table, have been synthesized already [2–4]. The central space of porphyrins can only accommodate ions having an atomic radius smaller than 0.201 nm [2–4]; thus, causing that in the porphyrinic complexes containing the larger ions, the metallic element must be located outside of the molecular plane. Similar to the size of the cation, the presence of massive axial ligands can either induce the loss of planarity or the structural deformation of the macrocycle. Furthermore, both peripheral and remaining pyrrole hydrogens as well as those allocated on the *methine* bridges can be exchanged by different chemical substituents to render an extraordinary family of compounds (Figure 1(b)).

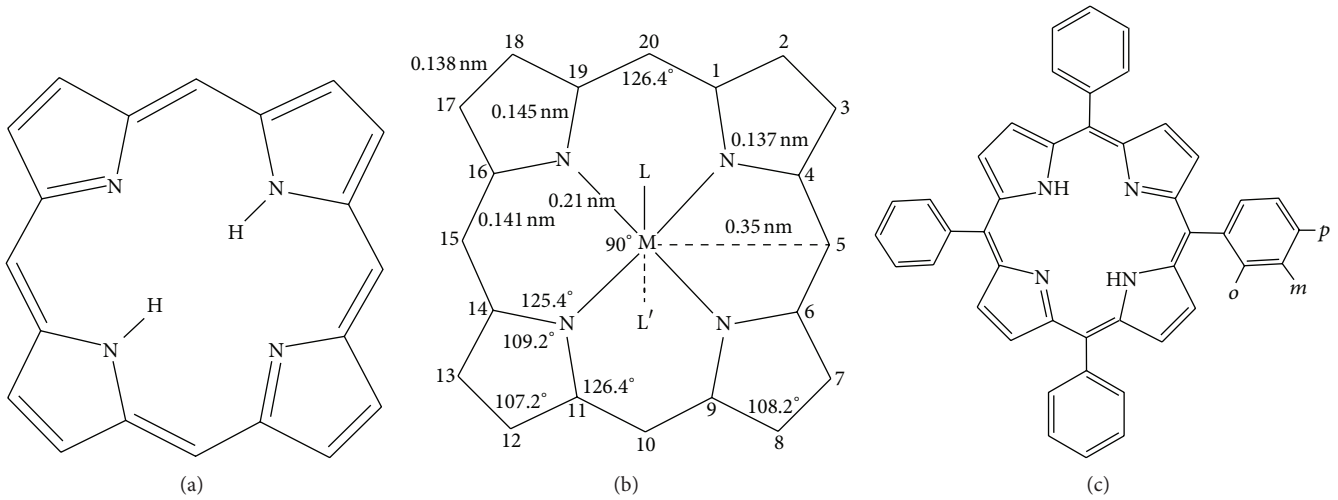


Figure 1: (a) Structure of the tetrapyrrolic porphin macrocycle; (b) bond lengths, bond angles, and positions (1 to 20) of possible peripheral substituents in the respective metallic complex; and (c) *ortho*-, *meta*-, and *para*-positions in a tetraphenylporphyrin ($H_2$T(*o*-, *m*-, *p*-S)PP).

The extensively delocalized $\pi$-electron systems of these centrosymmetric compounds confer upon them, besides chemical and thermal stability, some other interesting spectroscopic, optical, and electrical properties that allow a great number of applications in fields such as optics [5, 6], electrochemistry [7], catalysis [8], and sensoring [9, 10]. The free bases of porphyrins exhibit a red fluorescence in the range from 600 to 730 nm, and it is known that light of wavelength between 620 and 690 nm penetrates about 1.0 cm into biological tissues [11]. However, at both the far red or near infrared radiation regions (650 to 1,500 nm), a better tissue penetration occurs [12]. Furthermore, some substituted porphyrins are selectively adsorbed by malignant tissues when singlet oxygen ($^1O_2$) atoms are generated under red light illumination [2–4, 13–15]. Due to these properties, porphyrins have been extensively probed and used in Photodynamic Therapy (PDT) of cancer [16] and in the inactivation of some kinds of bacteria [17].

In *meso*-porphyrins, either one or several methylene hydrogens can be substituted by *alkyl* or *aryl* groups, as, for instance, phenyl rings in tetraphenylporphyrins ($H_2$TPP). In tetraphenylporphyrins, the substituents are commonly located at the *para*-positions of phenyls (Figure 1(c)); that is, these groups are situated on the same molecular plane [8, 18, 19]. It has been demonstrated that there exists a relationship among (i) the presence of electroattracting substituents, (ii) the basicity of the central nitrogens, and (iii) the *redox* and photophysical properties of $H_2$TPP molecules [20]. Reactivity differences have been discovered among the *ortho*-, *meta*-, and *para*-substituted isomers of tetrakis-(N-methylpyridinium)-porphyrin, $H_2TMPyP^{2+}$ [21, 22]. In this molecule, the *ortho*-isomer results to be a very acid porphyrin (pKa = −0.9), and it is a very well-known example of a stable porphyrin in acid medium (1 M), the $H_2TMPyP^{4+}$ dicationic form of which can be observed at high acid concentration (up of 10 M). Great differences in the redox and photophysical properties have been discovered among the *ortho*-, *meta*-, and *para*-halide substituted traphenylporphyrins, $H_2$T(o, *m ó p*-X)PP, and this kind of phenomenon has been termed as the "*ortho-effect*" [21–25].

The electroattracting character of the substituents present in *meso*-tetraphenylporphyrins diminish the intensity of UV-Vis absorption [21, 22, 26, 27], but this effect results are more evident in the emission spectra [23–25, 28]. Related to this, a shallow, but persistent shift is observed with respect of the principal bands (i.e., the Soret and *Q* bands) in the UV-Vis spectra of *para*-, *meta*-, and *ortho*-$H_2$TMPyP isomers. Yet, these changes occur differently for *ortho*- and *para*-isomers than for the *meta*-isomers. However, larger differences in the UV-Vis spectra are detected for the *ortho*, *meta*, and *para* isomers of protonated forms of $H_2$TPP and $H_2$TMPyP species.

For some of the above mentioned applications, porphyrins require to be trapped or fixed inside diverse substrates such as carbon, zeolites, and inorganic oxides [29]. However, the development of pertinent methods for preserving the physicochemical and luminescent properties of porphyrins trapped or fixed within polymer networks has been scarcely explored during the past decades [30–32]. In view of the transcendental role played by tetrapyrrole macrocycles in nature and because of the properties inherent in their synthetic analogues, during the last decade an increased interest has aroused for the synthesis of new materials based on the use of these compounds [4, 33–49]. At this concern, new polymeric systems were synthesized; the important point being that porphyrins could be trapped, fixed as a ramification, or inserted as part of the polymeric chain. The materials so obtained showed interesting physicochemical properties suitable to be used in technological areas and devices such as catalysis [4, 37, 38], electrocatalysis [31, 32], solar cells [4, 39, 40], electronics [4, 41], optics [4, 42, 43], permeable membranes [44], medical appliances [45, 46], and sensors [47–49].

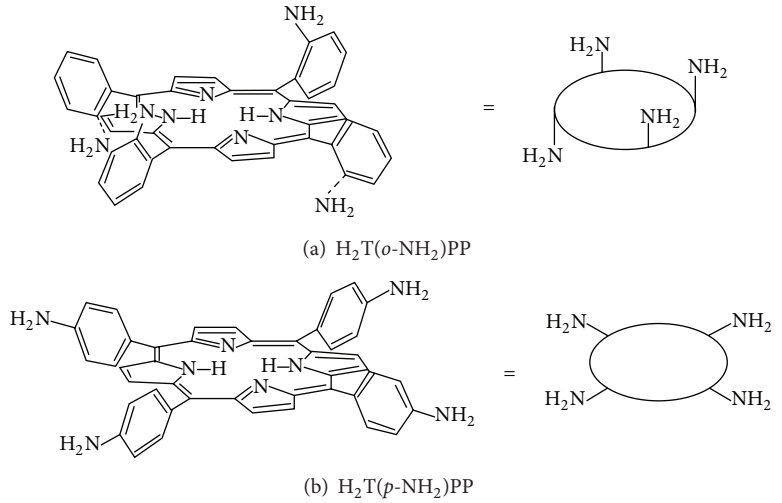

(a) $H_2T(o\text{-}NH_2)PP$

(b) $H_2T(p\text{-}NH_2)PP$

Figure 2: Structural representation of: (a) *ortho*-amino, $H_2T(o\text{-}NH_2)PP$, and (b) *para*-amino, $H_2T(p\text{-}NH_2)PP$, isomers of substituted tetraphenylporphyrins.

In the present work, we have explored the structural effect of structurally attaching different isomers of tetraphenylporphyrins over polymer fibbers that grow from polyamine Nylon 66-like polymers when the isomers of *ortho*- and *para*-amine substituted tetraphenylporphyrins, that is, ($H_2T$(o–$NH_2$)PP and $H_2T$(p–$NH_2$)PP) (Figure 2), were included in the synthesis. The formation of the respective cobalt complexes of porphyrins was used as a way to confirm and quantify the presence of it in the polyamide chains. The miscellaneous properties showed by porphyrins and their potential integration to Nylon 66 fibbers could be used in the design of new and interesting hybrid materials, suitable to be employed in assorted technological areas.

## 2. Experimental

*2.1. Synthesis of Porphyrin Free Bases.* Free bases of *ortho*-(*o*) and *para*-(*p*) substituted tetraphenylporphyrins, $H_2T$(*o*- or *p*-S)PP (Figure 1(b)), were synthesized by the Rothemund reaction and the Adler Method [50–52], from their respective substituted *ortho*- or *para*-nitro benzaldehyde, together with pyrrole, and zinc acetate, $Zn(Ac)_3$, under reflux in propionic acid (Figure 3). Once the reaction mixture was cooled to ambient conditions, an equivalent volume of chloroform was added to the mixture, which was kept under stirring for 12 hours. The resultant solid was filtered and washed with chloroform and methanol until the filtered liquid was clear. In a second step, the nitro groups ($-NO_2$) were reduced with a $SnCl_2{\cdot}2H_2O$, HCl solution while maintaining the temperature at around 65–70°C for 25 minutes. After this period, the mixture was neutralized with a 30 vol.% $NH_4OH$ solution. The reddish precipitate was extracted with chloroform, which was later evaporated. The solid obtained was washed with a diluted ammonia solution. Purified $H_2T(o\text{-}NH_2)PP$ or $H_2T(p\text{-}NH_2)PP$ solids were obtained by filtration through a chromatographic silica gel column employing chloroform as eluent. The resultant purple solids were characterized by elemental chemical analysis, FTIR, UV-Vis, and fluorescence spectroscopies.

*2.2. Synthesis of Nylon 66 with Chemically Attached Ortho- or Para-$NH_2$ Substituted Porphyrins (Ny 66-o-$NH_2$ or Ny 66-p-$NH_2$).* To synthesize Nylon 66 fibers containing free bases of porphyrins as part of the polyamide structure, 0.8 g of hexamethylene diamine was dissolved in 12 mL of a 0.625 M NaOH solution. This dissolution was added under continuous stirring to a second mixture consisting of 1 mL of adipoyl chloride and 11.1 mL of a solution of either $1.63 \times 10^{-4}$ M of $H_2T(o\text{-}NH_2)PP$ or $H_2T(p\text{-}NH_2)PP$, in chloroform, while kept under ice inside a water bath (Figure 4). The polyamide solid formed this way was filtered and washed with methanol and chloroform, dried at room temperature overnight, and left reacting for one more night at 75°C. For simplicity, the samples were labeled as Ny 66-*o*-$NH_2$ or Ny 66-*p*-$NH_2$; additionally, a pure Nylon 6 sample was synthesized in the absence of porphyrins to be employed as a blank specimen. All polyamides were characterized by FTIR, UV-Vis, fluorescence, SEM, and EDS mapping.

*2.3. Synthesis of the Ny 66-Co-o-$NH_2$ or Ny 66-Co-p-$NH_2$ Cobalt Complexes.* The Ny 66-Co-*o*-$NH_2$ or Ny 66-Co-*p*-$NH_2$ cobalt complexes were synthesized from a 0.100 g mixture of the respective Ny 66-*o*-$NH_2$ or Ny 66-*p*-$NH_2$ samples dissolved in methanol and 0.4 g of $CoCl_2$; this reactant system was kept under reflux for 12 h. After this time, the solids were filtered and washed sequentially with methanol, chloroform, and water to eliminate any unreacted cobalt. The dried solids were characterized by FTIR, UV-Vis, and fluorescence spectroscopies, as well as by HRSEM and EDS mapping.

*2.4. Instrumentation.* UV-vis-NIR characterization was carried out in a Cary-Varian 500 E spectrophotometer from

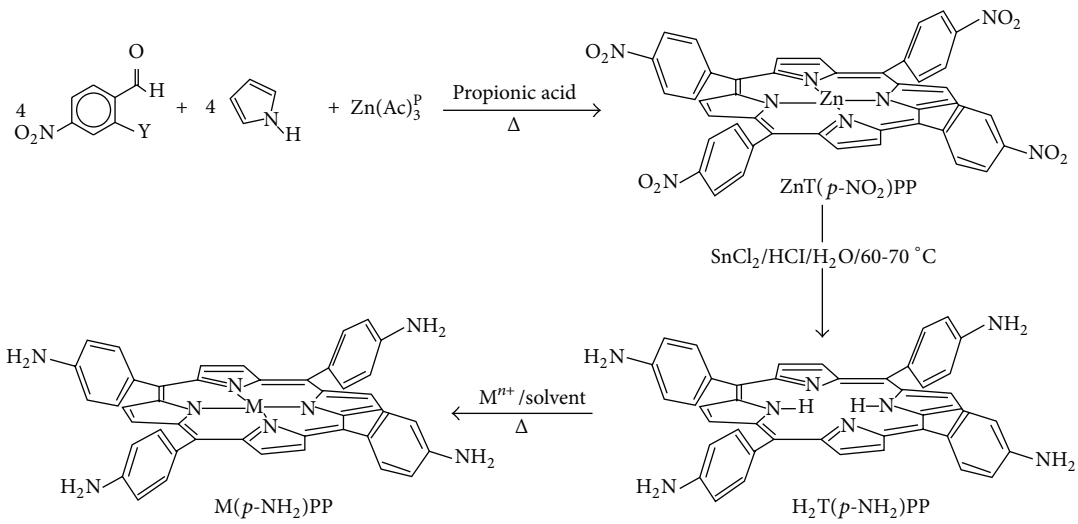


Figure 3: Synthesis route of $H_2T(p\text{-}NH_2)PP$ species through the production of $Zn(p\text{-}NO_2)PP$, zinc tetra-nitro-phenyl porphyrin, intermediary. Starting from the $H_2T(p\text{-}NH_2)PP$ free base, it is possible to synthesize complexes with some other cations ($M^{n+}$), including cobalt.

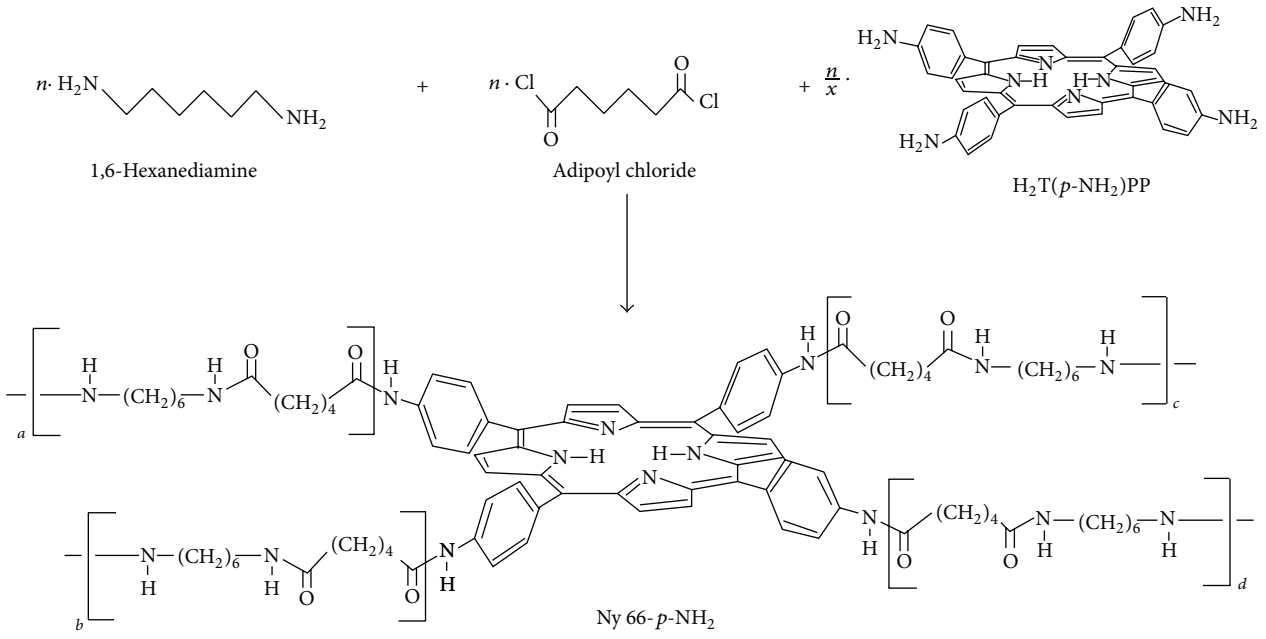


$a + b + c + d = n$, and $x \leq 4$

Figure 4: Synthesis route for the incorporation of the $H_2T(o\text{- or }p\text{-}NH_2)PP$ species into the Nylon 66 network; the $a$, $b$, $c$, and $d$ subindexes are related to the lateral chains formed over the amine groups of porphyrin, which could attain the same or different sizes.

200 to 800 nm (UV-vis) and from 1000 nm to 2500 nm (100,000 to 4,000 $cm^{-1}$) (NIR). Infrared spectra (FTIR) were obtained from a Perkin-Elmer GX FTIR spectrometer. The fluorescence of solutions was measured at 25°C in a PC1 spectrofluorometer from ISS (Champaign, IL), equipped with a water-jacketed cell holder for temperature control. Fluorescence emission of the hybrid solids was obtained at room temperature, between 200 and 800 nm (UV-vis), by means of a Perkin-Elmer 650-10S spectrofluorometer fitted with a 150 W xenon lamp. The XRD diffractograms were obtained with powders Diffractometer Siemens D-5000 with graphite monochromator of $\lambda(CuK\alpha) = 1.5418$ Å. HRSEM images were obtained from a JEOL 7600F Instrument, including an Oxford Instruments INCA EDS detector.

## 3. Results and Discussion

The UV-visible spectra of free porphyrins are characterized by an intense band at around 420–430 nm (i.e., the Soret or B band) and four small Q bands in the range from 500

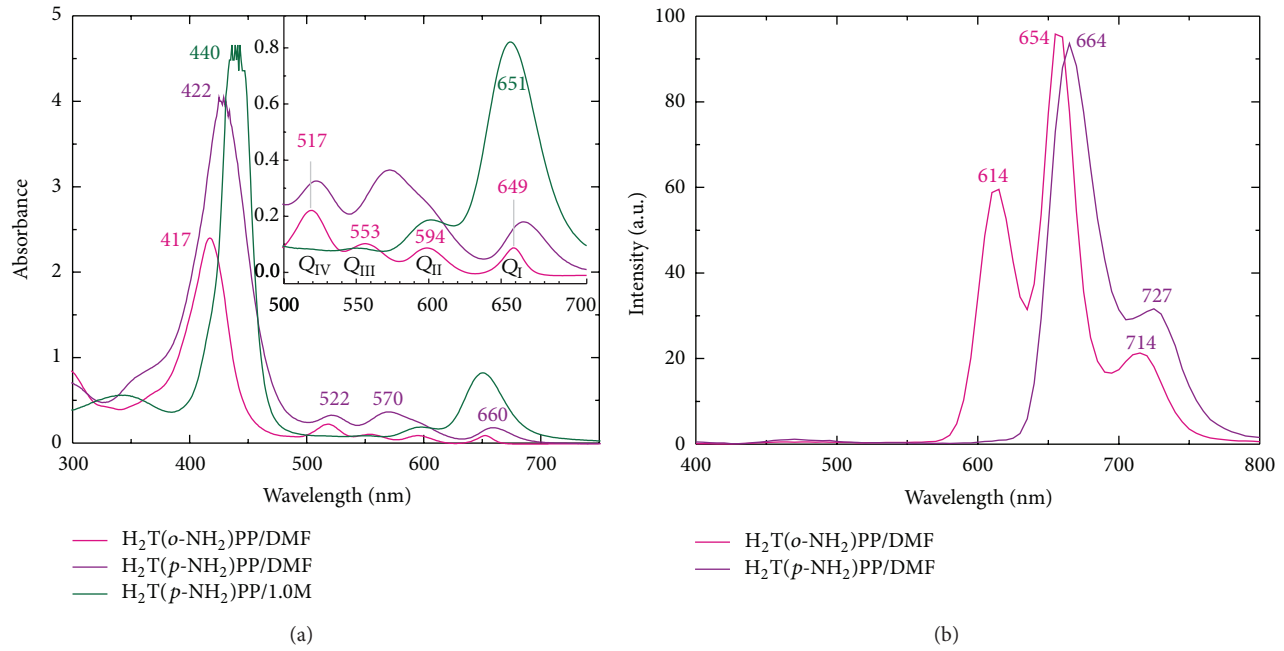


FIGURE 5: (a) UV-Vis and (b) fluorescence spectra ($\lambda_{exc}$ = 3270 nm) of $H_2T(o\text{-}NH_2)PP$ and $H_2T(p\text{-}NH_2)PP$ free bases and $H_4T(p\text{-}NH_2)PP^{2+}$ dicationic species in solution.

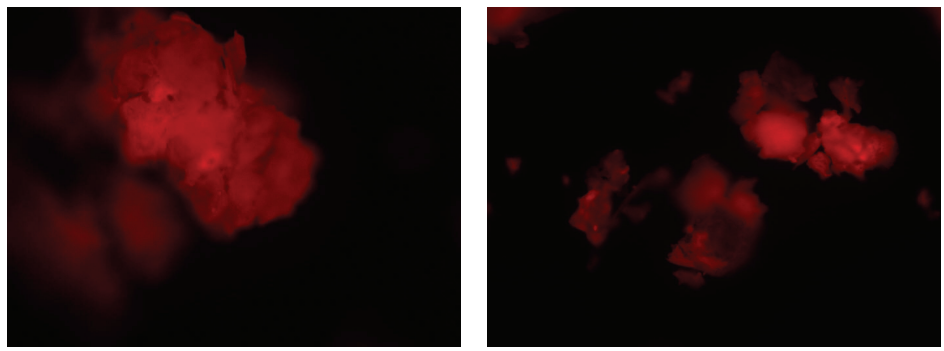


FIGURE 6: Microscopy images (×10) of the fluorescent: (a) Ny 66-$o$-$NH_2$ and (b) Ny 66-$p$-$NH_2$ samples.

to 700 nm; these last signals are assigned to the $a_{2u} \rightarrow e_g$ and $a_{1u}$, $a_{2u} \rightarrow e_g$ transitions, respectively [2, 3]. In acid solution, free porphyrins can be protonated to form the $H_4P^{2+}$ dicationic species. The UV-visible spectrum of this species shows a bathochromic-shifted Soret band (20–40 nm); the $Q_{IV}$ and $Q_{III}$ bands disappear, while the $Q_I$ signal grows and masks the $Q_{II}$ band [2, 3, 53]. Further changes evidence an increment in the resonance interaction between phenyl and pyrrolic rings followed by a slight projection out of the molecular plane of the compound [54].

For the particular case of $H_2T(o\text{-}NH_2)PP$ species in solution, the Soret band is observed at 417 nm together with four $Q$ bands at 517, 553, 594, and 649 nm (Figure 5(a)), respectively. In the case of the $H_2T(p\text{-}NH_2)PP$ species, the Soret band is located at 622 nm, while three other bands appear at 522, 570, and 660 nm, the $Q_{II}$ signal being a broad band at around 590 nm. In acid solution, the purple-red solution of these compounds turns green as a consequence of porphyrin protonation. The protonation of the central nitrogens of the porphyrin macrocycle leads to the formation of $H_4T(o\text{-}NH_2)PP^{2+}$ or $H_4T(p\text{-}NH_2)PP^{2+}$ dicationic species, the UV-vis spectra of which show bathochromic-shifted Soret bands, and lonely $Q_I$ bands that mask the remaining $Q$ bands. In the particular case of $H_2T(p\text{-}NH_2)PP$ species, the Soret band is observed at 440 nm and the $Q_I$ band at 651 nm. As it was mentioned in Section 1, many of the free bases of porphyrins and some of their complexes show fluorescence in the visible region, principally in the red part of the spectrum [8, 18, 19]. In turn, $H_2T(o\text{-}NH_2)PP$ or $H_2T(p\text{-}NH_2)PP$ solutions show fluorescence spectra with a principal

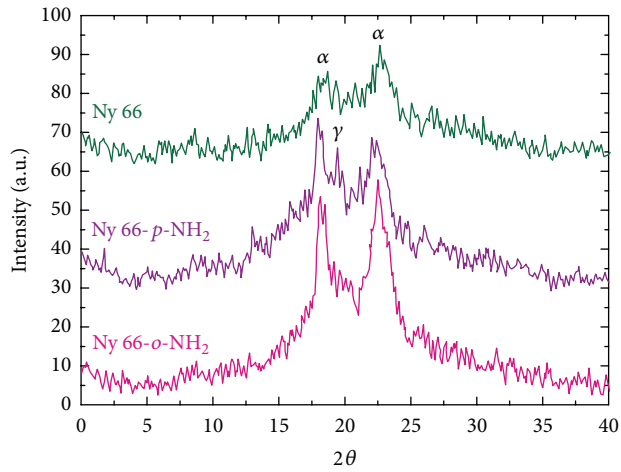


FIGURE 7: X-ray diffraction spectra of the Nylon 66, Ny 66-*o*-$NH_2$, and Ny 66-*p*-$NH_2$ samples.

band located at around 650 to 660 nm and a lesser intense band at around 710–730 nm (Figure 5(b)). Moreover, the $H_2T$(*o*-$NH_2$)PP species show an additional band at around 614 nm.

The optimization of the above mentioned methodology can render new materials suitable to be used in diverse technological fields as optics, catalysis, sensor, medicine, or inclusively in electronics if conductive polymers are incorporated.

After the synthesis and purification of Nylon 66 fibers containing *ortho*- or *para*-amine substituted porphyrins, the Ny 66-*o*-$NH_2$ and Ny 66-*p*-$NH_2$ final samples were obtained. These specimens were amorphous, granular, and yellowish solids. In these samples, it was possible to observe the characteristic red fluorescence of porphyrins after being subjected to UV irradiation (Figure 6).

The X-ray diffraction patterns (Figure 7) of the Nylon 66, Ny 66-*o*-$NH_2$, and Ny 66-*p*-$NH_2$ samples showed the same diffraction pattern of a predominant amorphous material with some crystallinity amount. In this sense, the bands at around 20.5° and 24.5° correspond to the reflection of (100) and (010, 110) doublet of the $\alpha$ phase of Nylon 66 crystals oriented in a triclinic cell, and the less intense band observed at around 21.6° in the diffractogram of the Ny 66-*p*-$NH_2$ could be assigned to the presence of $\gamma$ phase in this sample [55–57]. The couple of bands attributed to the $\alpha$ phase were more intense for the Ny 66-*o*-$NH_2$ and Ny 66-*p*-$NH_2$ samples than for the pristine Nylon 66. This difference and the existence of $\gamma$ phase in the Ny 66-*p*-$NH_2$ sample could be attributed to a slight crystallinity increment induced by the incorporation of the porphyrins in the polyamide network.

As for the FTIR spectrum of $H_2T$(*p*-$NH_2$)PP free base species (Figure 8), one band can be seen at around 3300 $cm^{-1}$ and another one at 960 $cm^{-1}$; these signals can be ascribed to the NH bond stretching and bending frequencies of $NH_2$ substituents and of the central nitrogens of the porphyrin free base. The bands located in the range from 2850 to 3150 $cm^{-1}$ are attributed to C–H bond vibrations of the benzene and pyrrole rings. The band located at around 1490 to 1650 $cm^{-1}$ can be assigned to C=C vibrations and that located at around 1350 and 1272 $cm^{-1}$ can be due to –C=N and C–N stretching vibrations. The signals at around 1800 to 1900 $cm^{-1}$ as well as the bands at about 800 $cm^{-1}$ and 750 $cm^{-1}$ are ascribed to C–H bond bending vibrations of *para*-substituted phenyls.

In the FTIR spectra of pure Nylon 66, it can be observed that the bands at 3314 and 3221 $cm^{-1}$ and those arising at 1450 $cm^{-1}$ and 750 $cm^{-1}$ can be assigned to the stretching, deformation, and wagging vibrations of N–H bonds. The bands at 3089 and 3020 $cm^{-1}$ are due to the asymmetric and symmetric stretching vibrations of C–H bonds. The bands at 2946 and 2867 $cm^{-1}$ are associated to the $CH_2$ stretching vibrations. In turn, the C=O stretching vibrations can be observed at around 1717 $cm^{-1}$. The stretching, asymmetric deformation, and wagging of NH amide groups are observed at 1654, 1547, and 1376 $cm^{-1}$, respectively. The bands located at around 1140 $cm^{-1}$ can be attributed to CO–CH symmetric bending vibration combined with $CH_2$ twisting. The bands at 936 and 600 $cm^{-1}$ are associated with the stretching and bending vibrations of C–C bonds, and the band at 583 $cm^{-1}$ can be due to O=C–N bending. The bands appearing at 936 and 1140 $cm^{-1}$ are associated to the crystalline and amorphous structures of Nylon 66, respectively [58]. In the spectra of polymers containing *ortho*- or *para*-isomers of porphyrin, that is, Ny 66-*o*-$NH_2$ and Ny 66-*o*-$NH_2$, the bands in the range from 3100 to 3600 $cm^{-1}$ are slightly narrower than those observed in Nylon 66 spectra, suggesting a lower amount of physisorbed water. The bands located at around 3150 and 3300 $cm^{-1}$ suggest the presence of a very low amount of macrocycle molecules in the solid samples. Furthermore, the band at around 940 $cm^{-1}$ appears to have a lower intensity in the Ny 66-*o*-$NH_2$ system, thus suggesting a lower crystalline structure than that of the Ny 66-*p*-$NH_2$ sample. Because of the low concentration of macrocyclic species that are incorporated into the polymer network, the last result may not be conclusive at this point.

In the UV-vis spectra of Nylon 66 synthesized altogether with the $H_2T$(*o*-$NH_2$)PP, $H_2T$(*p*-$NH_2$)PP species (samples labelled as Ny 66-*o*-$NH_2$ and Ny 66-*p*-$NH_2$), the band at around 250 nm and the shoulder at 290 nm, assigned to the Nylon 66 [59], are observed to depict a lower intensity than those due to the intense $\pi$-$\pi^*$ transitions of porphyrins. By this reason, the UV-Vis analysis is centred to the signals of the macrocyclic species. In the Ny 66-*o*-$NH_2$ and Ny 66-*p*-$NH_2$ samples, the observed Soret bands were wider than those obtained from solutions of these macrocycles and located at 437 and 426 nm, respectively (Figure 9). Both samples show the four *Q* bands, characteristic of porphyrin free base, however, the red-shifted Soret band together with the $Q_I$ band (at 656 nm) in the spectrum of Ny 66-*o*-$NH_2$ suggests the existence of a very small concentration of protonated porphyrin, that is, and likely, a higher interaction with the polyamide chains. The shift of the Soret band in the case of Ny 66-*p*-$NH_2$ was of only 4 nm, thus suggesting a low interaction of the macrocycle with the polyamide chains.

In the fluorescence spectra of Nylon 66 synthesized together with $H_2T$(*o*-$NH_2$)PP or $H_2T$(*p*-$NH_2$)PP species,

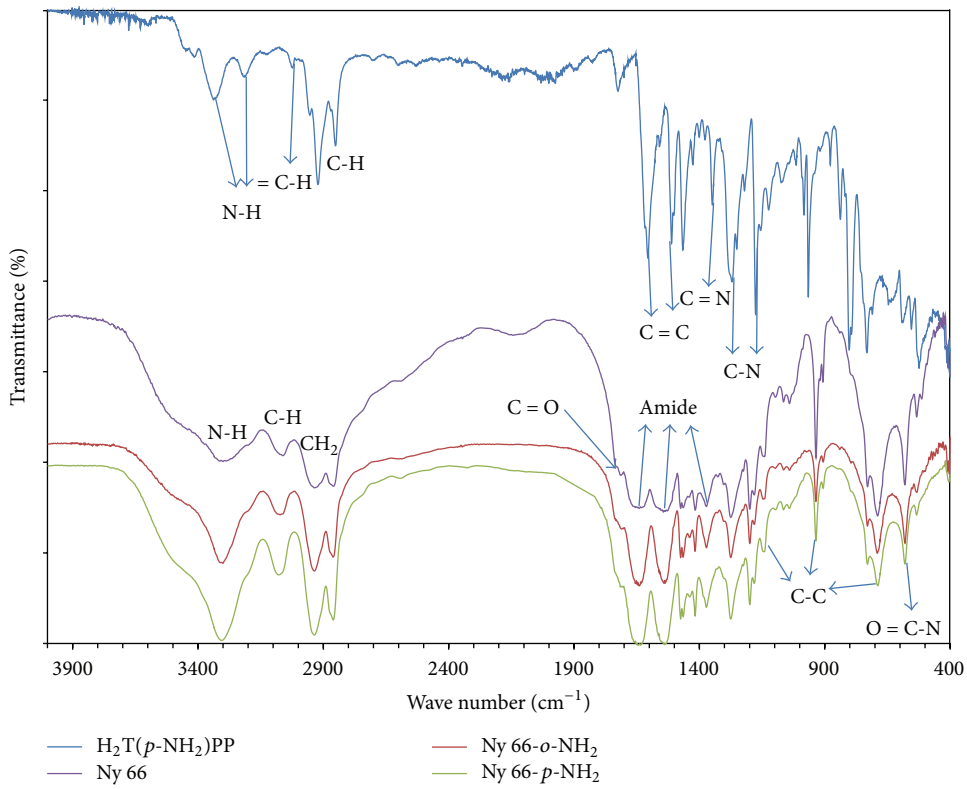


Figure 8: FTIR spectra of pure Nylon 66 (blank) and of Ny 66-*o*-$NH_2$ and Ny 66-*p*-$NH_2$ hybrid species as compared with the FTIR spectrum of the $H_2T$(*p*-$NH_2$)PP free base.

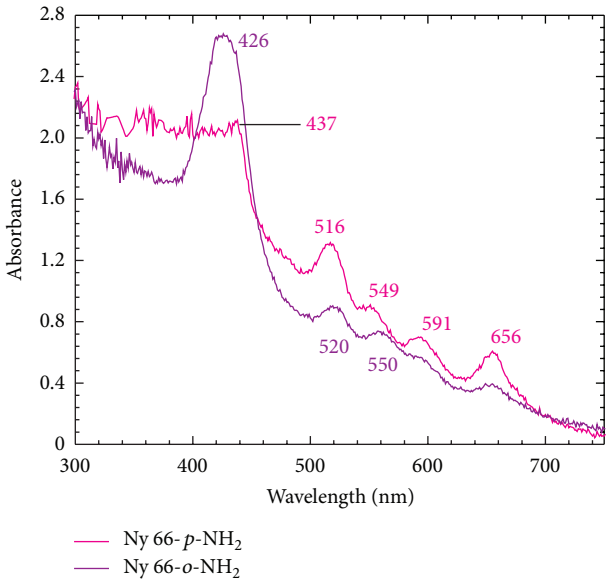


Figure 9: UV-Vis spectra of dry Ny 66-*o*-$NH_2$ and Ny 66-*p*-$NH_2$ samples.

obtained by excitation at 370 nm ($\lambda_{exc}$ = 370 nm), two set of signals can be observed (Figure 10(a)); the bands located at around 661 and 674 nm can be due to the fluorescent red emission of $H_2T$(*o*-$NH_2$)PP and $H_2T$(*p*-$NH_2$)PP free bases, respectively [60–62]. As it was demonstrated for Nylon 66, both, samples show fluorescence and phosphorescence; these phenomena can be attributed to the presence of chromophoric structures or oxidation impurities created during the synthesis of the polymers [63–67]. Then, the bands seen in the range from 380 to 600 nm with maxima appearing at 461, 471, and 532 nm can be the result of the emissions of polyamide alone [63–67] or from its interaction with the macrocycle species. When these spectra are obtained by using an exciting light of 420 nm, that is, in the range of maximum absorbance, the signals appearing in the interval from 430 to 600 nm are observed to depict a lower intensity than those signals located from 600 to 750 nm (Figure 10(b)). This means that bands displayed from 600 to 750 nm are emissions that can only be associated to the macrocyclic species, while the emissions of pure polyamide, or its interaction with the macrocycle, can only be observed when the systems are irradiated with light of a higher energy of shorter wavelength (i.e., $\lambda_{ex} \approx 370$ nm). Additionally, this last observation means that, in the synthesized systems, macrocyclic species and polyamide chains remain in the proximity of one another.

Even if the shape and localization of the bands in these last spectra are very similar to those observed for porphyrins in solution (Figure 5(b)), in the case of the Ny 66-*o*-$NH_2$ sample, the maximum band at 661 nm is red-shifted by about 7 nm and the band at 724 nm is red-shifted by 10 nm with respect to those observed in solution (Figure 5(b)). Furthermore, in this sample, the third band appearing at 614 nm, in the spectra of the $H_2T$(*o*-$NH_2$)PP solution, appears very weakly and at the same position as for the Ny 66-*o*-$NH_2$ sample.

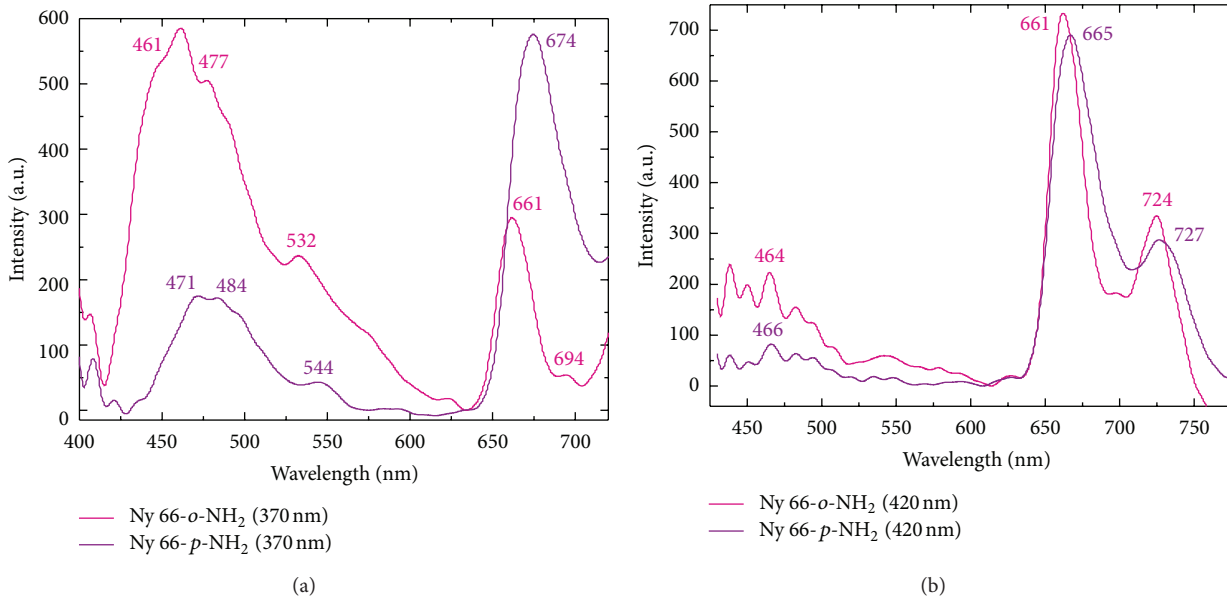


FIGURE 10: Fluorescence spectra obtained with excitation radiation of 370 nm (a) or 420 nm (b) of the Ny 66-*o*-$NH_2$ and Ny 66-*p*-$NH_2$ samples.

The bands in the fluorescence spectra of the Ny 66-*p*-$NH_2$ sample remain practically at the same positions than those observed for the porphyrin in solution, that is, located at 665 and 727 nm. The last observations suggest that, in the Ny 66-*p*-$NH_2$ sample, porphyrin remains immersed under a physicochemical environment that is practically not affecting its emission process. Comparatively, the fluorescence spectra of the Ny 66-*o*-$NH_2$ sample suggest that, in this network, the luminescent process of porphyrin is slightly affected by the proximity of the polyamide chains formed up and down of the macrocycle plane, then causing that the emissions occur at longer wavelengths than those found in solution. That is, under these conditions, the emission of the $H_2$T(*o*-$NH_2$)PP species takes place after dispersing some amount of energy through vibration, something that is facilitated by the presence of polyamide chains.

The examination of the characteristic UV-Vis and fluorescence bands in the spectra of the Ny 66-*o*-$NH_2$ and Ny 66-*p*-$NH_2$ samples confirms the incorporation of a low amount of the respective $H_2$T(*o*-$NH_2$)PP and $H_2$T(*p*-$NH_2$)PP species into the structure of the polyamide network.

In the SEM images of Nylon 66, synthesized as a blank, both layered and radial structures can be observed of approximately the same diameters of about 7 $\mu$m (Figures 11(a) and 11(b)). In contrast, the images of polyamide synthesized in the presence of the $H_2$T(*o*-$NH_2$)PP species show lamellar and curved structures in which the radial structures, observed in the blank sample, cannot be furthermore detected (Figures 11(c) and 11(d)). Additionally, in the polymer synthesized in the presence of the $H_2$T(*p*-$NH_2$)PP species, there exists a rougher but more homogeneous, compact, and complex structure. This structure consists of a sequence of continuous and folded layers inside a network with, apparently, a higher amount of smaller pores (Figures 11(e) and 11(f)). Evidently, in the cases of these systems, the presence of porphyrin isomers induces particular textural effects.

As it is well known, porphyrin macrocycles are tetradentate agents which form complexes with practically all metallic elements of the periodic table [2–4]. In order to probe the existence and evaluate the amount of porphyrin macrocycle integrated to the structure of polyamide, the preparation of the respective cobalt complexes was performed. For example, the UV-Vis spectra of the CoT(*p*-$NH_2$)PP complex in solution (Figure 12(a)) show an intense Soret band, shifted to longer wavelengths located at 438 nm. In the region of *Q* bands, the $Q_{III}$ and $Q_{II}$ bands remain situated at around 555 and 597 nm. The last pathway of signals is characteristic of porphyrinic complexes [2–4]. In the respective UV-Vis spectra of samples of Nylon 66 synthesized with $H_2$T(*o*-$NH_2$)PP or $H_2$T(*p*-$NH_2$)PP and obtained after the reaction with $CoCl_2$, signals of porphyrinic complexes formation are observed. In both cases, the detected Soret bands are of a high intensity, broad, red-shifted, and located at 442 and 451 nm for the samples labeled as Ny 66-Co-*o*-$NH_2$ and Ny 66-Co-*p*-$NH_2$, respectively (Figure 12(b)). In the spectrum of the last sample, only the $Q_{III}$ and $Q_{II}$ bands are observed at around 550 and 592 nm. For the case of Ny 66-Co-*o*-$NH_2$ sample, the $Q_{III}$ and $Q_{II}$ bands are observed as shoulders at around and 549 nm. The bands displayed in the spectra of the two systems confirm the formation of the respective complexes by substitution of the two central hydrogens of porphyrin by cobalt ions. However, the deformation of the pathway of these bands may be attributed to the interactions of cobalt porphyrins with polyamide chains. The amount of cobalt integrated to the polymeric systems results is lower for the system synthesized with the $H_2$T(*o*-$NH_2$)PP species, while this same amount was higher for the polymer containing the $H_2$T(*p*-$NH_2$)PP species.

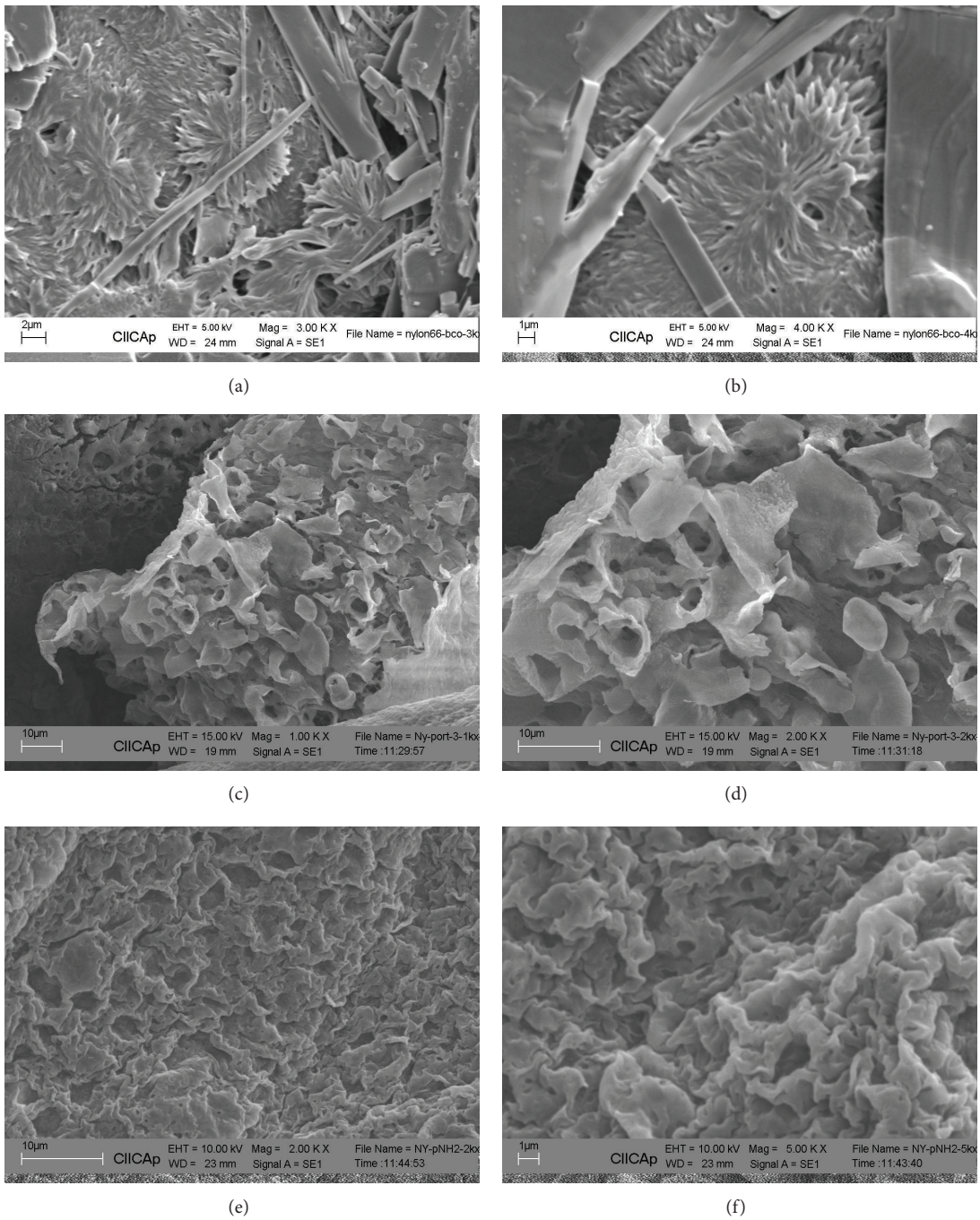


Figure 11: SEM images of Nylon-66 ((a) and (b)), Ny 66-*o*-$NH_2$ ((c) and (d)) and, Ny 66-*p*-$NH_2$ ((e) and (f)) samples.

From the EDS analysis of Ny 66-Co-*o*-$NH_2$, a uniform distribution of carbon (Figure 13(b)) is evident; contrastingly, the nitrogen distribution (Figure 13(c)) follows a pathway that coincides with the borders of the curved layers observed in the SEM micrograph (Figure 13(a)). The carbon distribution can be associated to the six carbons existing in adipic acid and hexane diamine chains that are present in the polyamide chains and also with the carbon skeleton of porphyrins. However, the nitrogen distribution can only be associated to the nitrogens of amide groups, to the four central porphyrinic nitrogens, and to the four peripheral nitrogens, attached at the *ortho-* or *para*-positions of phenyls in the macrocycle.

The amount of cobalt detected in the Ny 66-Co-*o*-$NH_2$ and Ny 66-Co-*p*-$NH_2$ systems is very low (Table 1); nevertheless, it allows to calculate the approximated amount of monomer units present in every material. Having that in mind, the cobalt complex formed with a porphyrin macrocycle has the molecular formula $CoC_{44}H_{32}N_8$, and four chains of the same length can be formed from the *ortho-* or *para*-$NH_2$ groups attached at the periphery of macrocycle;

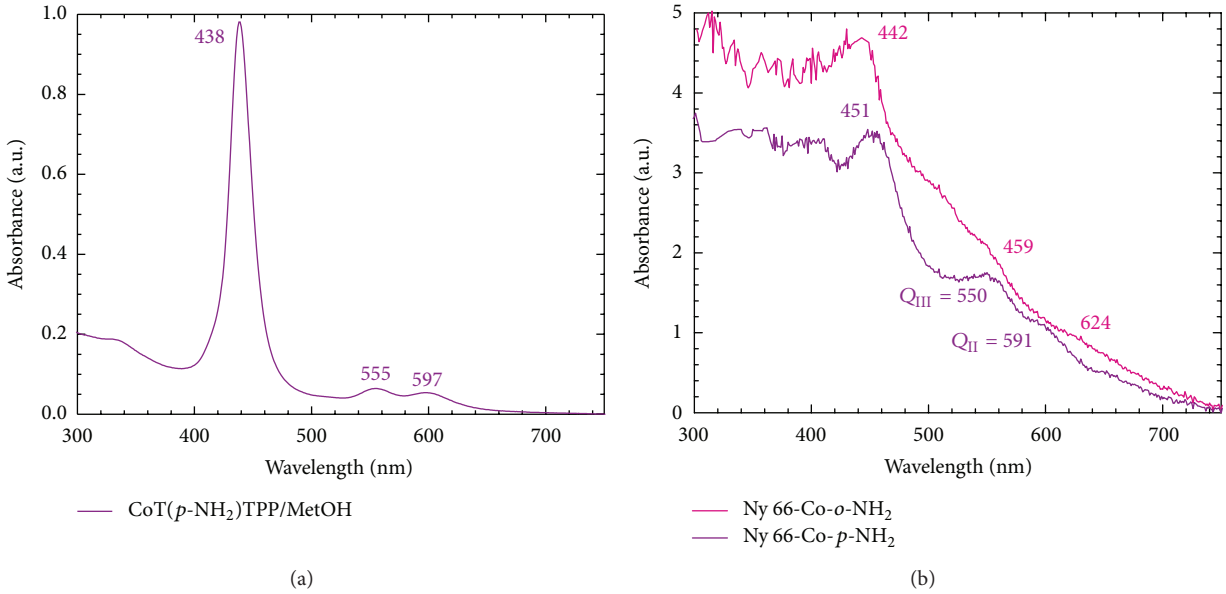


FIGURE 12: (a) UV-Vis spectra of CoT($p$-$NH_2$)PP in solution and of the (b) Ny 66-Co-$o$-$NH_2$ and Ny 66-Co-$p$-$NH_2$ polymers.

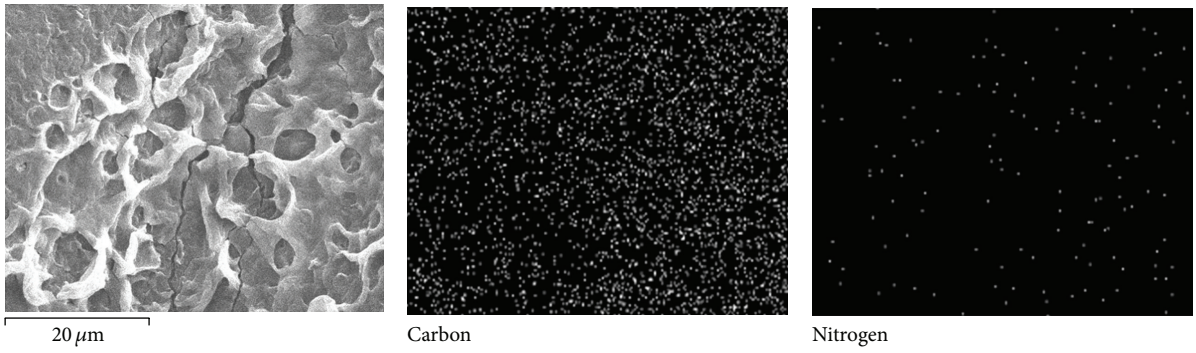


FIGURE 13: (a) SEM image and EDS distributions of (b) Carbon and (c) Nitrogen on the surface of the Ny 66-Co-$o$-$NH_2$ sample.

the weight percent evaluated from the EDS analysis allows to determine that four chains are formed each consisting of 93 to 94 monomer units around every CoT($o$-$NH_2$)PP macrocycle. These chains are formed by around 78 monomeric units, in the case of CoT($p$-$NH_2$)PP (Table 1).

Because of the lower basicity of the –$NH_2$ groups attached in the $H_2$T($o$-$NH_2$)PP and $H_2$T($o$-$NH_2$)PP species, compared with the basicity of the hexanediamine, the formation of the Nylon 66 takes place faster and in a more easy way. However, the above mentioned results suggest that, in presence of the porphyrins, the formation of polyamide chains occurs easily with the $H_2$T($o$-$NH_2$)PP species, in which there exist two amine groups above and two other below the molecular plane. The integration of the porphyrins to the polyamide chains occurs began, or ending, on the –$NH_2$ groups, with the interactions between the two polyamide chains arising as in pristine Nylon 66. This situation makes the incorporation of additional porphyrin macrocycles between the same two chains difficult (Figure 14(a)), which probably takes place only with one of the two chains that grows at every side of the molecular plane of the $H_2$T($o$-$NH_2$)PP species. By these effects resulting rare the incorporation of another porphyrin with two shared chains of the four polyamide chains grow from every $H_2$T($o$-$NH_2$)PP species. By the same reasons, the length of the lateral chains formed around the $H_2$T($o$-$NH_2$)PP species is longer and has a low porphyrin concentration than those evaluated in the Ny 66-$p$-$NH_2$ sample. The polymerization of the four polyamide chains begins from the $H_2$T($p$-$NH_2$)PP species which occurs with lower steric hindrance existing around the four peripheral –$NH_2$ groups attached and localized in the same molecular plane of porphyrin (Figure 14(b)). The hydrogen and dipole-dipole interactions of amide groups are the principal responsible of the macroscopic structure of the formed polyamide network, with the $H_2$T($o$-$NH_2$)PP or $H_2$T($p$-$NH_2$)PP species determining only the initial growing and particular spatial disposition of polyamide chains. Perhaps, by this reason, the macroscopic structure of polyamide contained in $H_2$T($p$-$NH_2$)PP results to be rougher, denser, and with smaller pores

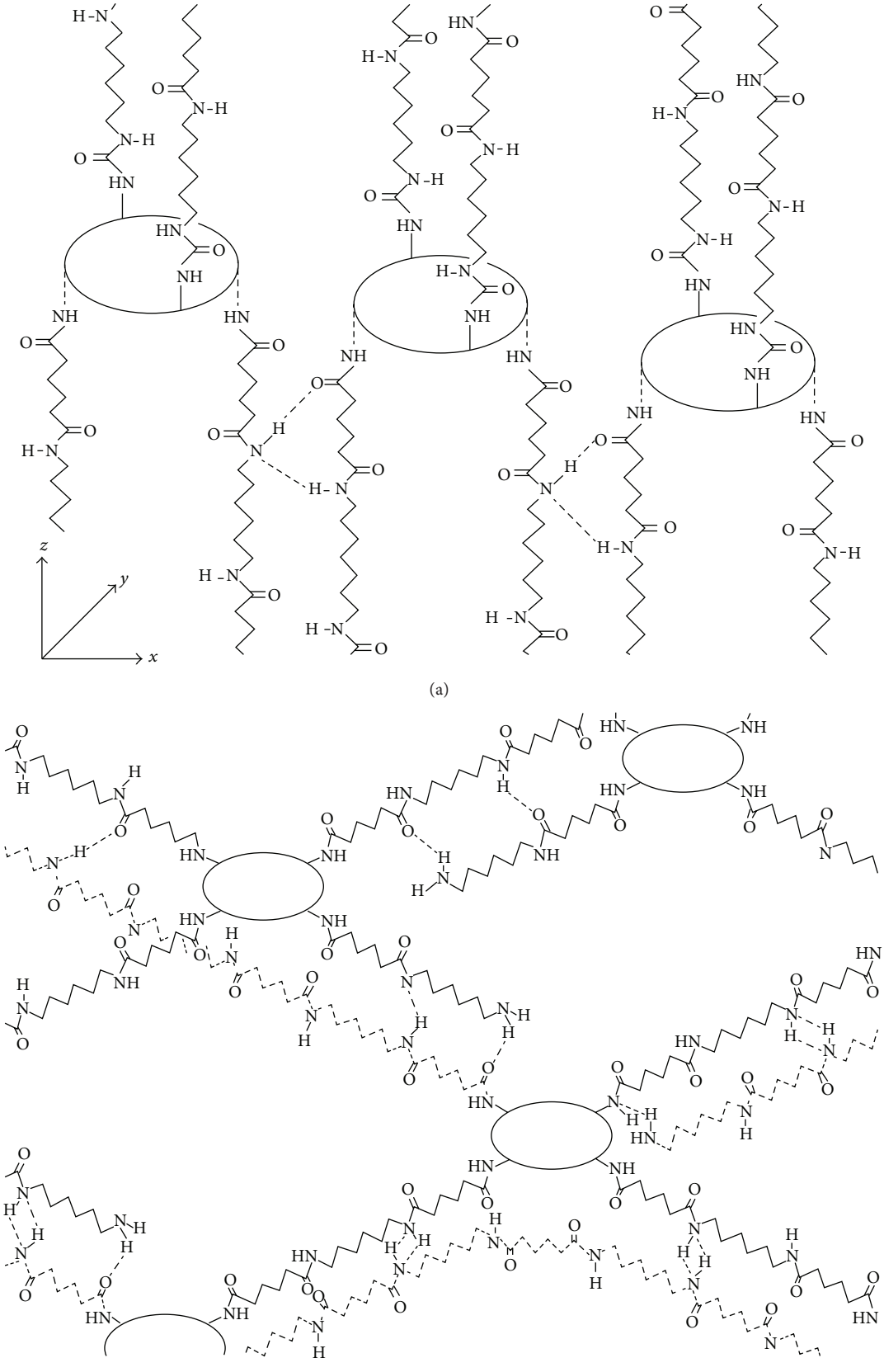


(a)

(b)

Figure 14: The spatial position of amine groups in *ortho*- or *para*-$NH_2$ substituted tetraphenyl porphyrins induces the growth of different pathways on Nylon 66 fibers.

Table 1: Weight % of carbon, oxygen, and cobalt evaluated by EDS on the surface of Ny 66-Co-*o*-$NH_2$ and Ny 66-Co-*p*-$NH_2$ samples.

| Sample | % w/w Carbon | % w/w Oxygen | % w/w Cobalt | Monomer units (*n*) | Number of units bilateral chain* |
|---|---|---|---|---|---|
| Ny 66-Co-*o*-$NH_2$ | 83.24 | 16.67 | 0.09 | 376 | 94 |
| Ny 66-Co-*p*-$NH_2$ | 77.57 | 21.33 | 0.10 | 312 | 78 |

*Lateral chains are formed by *a*, *b*, *c*, or *d* units rendering a total of *n* units in each porphyrin.

than those obtained with $H_2T$(*o*-$NH_2$)PP (Figures 11(b) and 11(c)).

All the above mentioned evidence suggests that the spatial localization of amine groups in the *ortho*- and *para*-amine substituted tetraphenylporphyrins induces important effects on the length, spatial disposition, and on the crossing and linking of polyamine chains. Furthermore, the polymerization occurs in such way that starts or ends over the –$NH_2$ groups of the $H_2T$(*o*-$NH_2$)PP or $H_2T$(*p*-$NH_2$)PP species. In the case of the $H_2T$(*o*-$NH_2$)PP species, the polyamide chains can be formed above and below of the molecular plane (along the *z*-axis direction in Figure 14(a)). In the case of $H_2T$(*p*-$NH_2$)PP, these chains can be formed at the periphery of the macrocycle (i.e., the *x*-*y* plane in Figure 14(b)). In the two cases, hydrogen bonds and dipole-dipole interactions between polyamide chains are responsible for the macroscopic structure of the polymer.

UV-Vis and fluorescence spectra suggest that polyamide chains interact stronger with the $H_2T$(*o*-$NH_2$)PP species than with the $H_2T$(*p*-$NH_2$)PP species. Additionally, the formation of cobalt complexes is more effective and in a higher amount, in the case of the network synthesized from $H_2T$(*p*-$NH_2$)PP, thus suggesting the existence of weak inhibiting effects over the central window of the macrocycle to coordinate cobalt or other cations. The last results suggest that the preferred direction for the growing of polyamide chains is initially determined by the position of the –$NH_2$ groups on the porphyrin. That is, the porphyrin macrocycle functions as a nucleation point (knot) that reinforces the Nylon structure and inhibits the formation of very long polyamide chains, but without creating a great interference with hydrogen bonds and dipole-dipole intermolecular interactions.

The above results suggest the incorporation of only a low amount of porphyrin molecules but still enough to display a notable fluorescence emission (Figures 6 and 10) and to form detectable amounts of cobalt atoms coordinated to the porphyrin structure. However, the possibility of increase the basicity of the –$NH_2$ groups of the $H_2T$(*o*-$NH_2$)PP or $H_2T$(*p*-$NH_2$)PP species exist for optimiz its integration to the polyamide chains. In a deeper investigation of the effect of using *ortho*- or *para*-substituted porphyrins on the structure of polyamides, our research group is now exploring the consequences of employing other porphyrin substituents or of other polyamide monomers, such as aromatic diamines or dicarboxyls. This possibilities suggest that the method can be optimized to a higher degree in order to synthesize new materials suitable to be used in optics, catalysis, sensors, membranes, medicine, and, if conductive polymers are included, in photoelectronic.

## 4. Conclusions

The results of the present document show that the incorporation of tetrapyrrole macrocyclic species is possible, such as the substituted porphyrins, in the structure of known polymeric chains such as Nylon 66. The integration of substituted porphyrinic molecules with spatial functional groups for the growing of polyamide chains induces beneficial structural and textural effects on the Nylon 66 matrix.

The number and spatial position of the amine groups (–$NH_2$) at the *ortho*- and *para*-positions of phenyls of tetraphenylporphyrins, incorporated to the polymerization reaction of adipoyl chloride and hexanediamine, produce two different modified Nylon networks. The use of $H_2T$(*p*-$NH_2$)PP species apparently induces the formation of a more homogeneous but rougher porous matrix than that of the $H_2T$(*o*-$NH_2$)PP species. However, the existence of four central nitrogens in the porphyrin macrocycle makes the synthesis of the respective cobalt complexes possible; these systems are suitable of be used with other cations such as transition metals, lanthanides, and actinides.

The optimization of the above mentioned methodology can render new materials suitable to be used in diverse technological fields as optics, catalysis, sensor, medicine, or inclusively in electronics if conductive polymers are incorporated.

## Acknowledgments

The authors wish to thank the CONACyT for the scholarship 252086 and the Ministry of Education (SEP-PROMEP) for the support provided to the Academic Body "Fisicoquímica de Superficies" (UAM-I CA-031) and to the Academic Network "Diseño Nanoscópico y Textural de Materiales Avanzados". The authors are grateful to Patricia Castillo for her timely and professional assessment at different stages of this investigation and Dr. Fernando Rojas-González for the review and comments of the different versions of the manuscript.

## References

[1] R. L. Milgrom, *The Colour of Life: An Introduction to the Chemistry of Porphyrins and Related Compounds*, Oxford University Press, Oxford, UK, 1997.

[2] K. M. Smith, *Porphyrins andMetalloporphyrins*, Elsevier Scientific Publishing, Amsterdam, The Netherlands, 1976.

[3] D. Dolphin, *The Porphyrins, Physical Chemistry, Part A and B*, Academic Press, New York, NY, USA, 1979.

[4] K. Kadish, K. M. Smith, and R. Guilard, *The Porphyrin Handbook*, vol. 6, Academic Press, San Diego, Calif, USA, 2003.

[5] J. Friedrich, H. Wolfrum, and D. Haarer, "Photochemical holes: a spectral probe of the amorphous state in the optical domain," *The Journal of Chemical Physics*, vol. 77, no. 5, pp. 2309–2316, 1982.

[6] J. Friedrich, H. Wolfrum, and D. Haarer, "Direct measurements of nonlinear absorption and refraction in solutions of phthalocyanines," *Applied Physics B*, vol. 54, no. 1, pp. 46–51, 1992.

[7] Y. Liu, K. Shigehara, and A. Yamada, "Preparation of Bis(phthalocyaninato)lutetium with various substituents and their electrochemical properties," *Bulletin of the Chemical Society of Japan*, vol. 65, pp. 250–257, 1992.

[8] J. R. Darwent, P. Douglas, A. Harriman, G. Porter, and M.-C. Richoux, "Metal phthalocyanines and porphyrins as photosensitizers for reduction of water to hydrogen," *Coordination Chemistry Reviews*, vol. 44, no. 1, pp. 83–126, 1982.

[9] A. D. F. Dunbar, S. Brittle, T. H. Richardson, J. Hutchinson, and C. A. Hunter, "Detection of volatile organic compounds using porphyrin derivatives," *Journal of Physical Chemistry B*, vol. 114, no. 36, pp. 11697–11702, 2010.

[10] H. Zhang, Y. Sun, K. Ye, P. Zhang, and Y. Wang, "Oxygen sensing materials based on mesoporous silica MCM-41 and Pt(II)-porphyrin complexes," *Journal of Materials Chemistry*, vol. 15, no. 31, pp. 3181–3186, 2005.

[11] S. Wan, J. A. Parrish, R. R. Anderson, and M. Madden, "Transmittance of nonionizing radiation in human tissues," *Photochemistry and Photobiology*, vol. 34, no. 6, pp. 679–681, 1981.

[12] J. P. A. Marijnissen and W. M. Star, "Quantitative light dosimetry *in vitro* and *in vivo*," *Lasers in Medical Science*, vol. 2, no. 4, pp. 235–242, 1987.

[13] A. Harriman, "Luminescence of porphyrins and metalloporphyrins—part 1: zinc(II), nickel(II) and manganese(II) porphyrins," *Journal of the Chemical Society, Faraday Transactions 1*, vol. 76, pp. 1978–1985, 1980.

[14] A. Harriman, "Luminescence of porphyrins and metalloporphyrins—part 2: copper(II), chromium(III), manganese(III), iron(II) and iron(III) porphyrins," *Journal of the Chemical Society, Faraday Transactions 1*, vol. 77, no. 2, pp. 369–377, 1981.

[15] A. Harriman, "Luminescence of porphyrins and metalloporphyrins—part 3: heavy-atom effects," *Journal of the Chemical Society, Faraday Transactions 2*, vol. 77, no. 7, pp. 1281–1291, 1981.

[16] E. Weizman, C. Rothmann, L. Greenbaum et al., "Mitochondrial localization and photodamage during photodynamic therapy with tetraphenylporphines," *Journal of Photochemistry and Photobiology B*, vol. 59, no. 1–3, pp. 92–102, 2000.

[17] E. Reddi, M. Ceccon, G. Valduga et al., "Photophysical properties and antibacterial activity of meso-substituted cationic porphyrins," *Photochemistry and Photobiology*, vol. 75, no. 5, pp. 462–470, 2002.

[18] A. Harriman, G. Porter, and P. Walters, "Photo-oxidation of metalloporphyrins in aqueous solution," *Journal of the Chemical Society, Faraday Transactions 1*, vol. 79, no. 6, pp. 1335–1350, 1983.

[19] A. Harriman, G. Porter, and M.-C. Richoux, "Photosensitised reduction of water to hydrogen using water-soluble zinc porphyrins," *Journal of the Chemical Society, Faraday Transactions 2*, vol. 77, no. 5, pp. 833–844, 1981.

[20] J. Turay and P. Hambright, "Activation parameters and a mechanism for metal-porphyrin formation reactions," *Inorganic Chemistry*, vol. 19, no. 2, pp. 562–564, 1980.

[21] P. Hambright, T. Gore, and M. Burton, "Synthesis and characterization of new isomeric water-soluble porphyrins. Tetra(2-N-methylpyridyl)porphine and tetra(3-N-methylpyridyl)porphine," *Inorganic Chemistry*, vol. 15, no. 9, pp. 2314–2315, 1976.

[22] J. B. Reid and P. Hambright, "Kinetics of copper incorporation into tetra(2-N-methylpyridyl)porphine. Effects of basicity on rate," *Inorganic Chemistry*, vol. 16, no. 4, pp. 968–969, 1977.

[23] J. B. Kim, J. J. Leonard, and F. R. Longo, "A mechanistic study of the synthesis and spectral properties of meso-tetraphenylporphyrin," *Journal of the American Chemical Society*, vol. 94, no. 11, pp. 3986–3992, 1972.

[24] D. J. Quimby and F. R. Longo, "Luminescence studies on several tetraarylporphins and their zinc derivatives," *Journal of the American Chemical Society*, vol. 97, no. 18, pp. 5111–5117, 1975.

[25] G. D. Egorova, V. N. Knyukshto, K. N. Solovev, and M. P. Tsvirko, "Intramolecular spin-orbital perturbations in ortho- and meta-halogeno-derivatives of tetraphenylporphin," *Optics and Spectroscopy*, vol. 48, no. 6, pp. 602–607, 1980.

[26] S. Sugata, S. Yamanouchi, and Y. Matsushima, "Meso tetrapyridylporphins and their metal complexes. Syntheses and physico chemical properties," *Chemical and Pharmaceutical Bulletin*, vol. 25, no. 5, pp. 884–889, 1977.

[27] M. Meot-Ner and A. D. Adler, "Substituent effects in noncoplanar $\pi$ systems. ms-porphins," *Journal of the American Chemical Society*, vol. 97, no. 18, pp. 5107–5111, 1975.

[28] G. D. Egorova, V. N. Knyukshto, K. N. Solovev, and M. P. Tsvirko, *Optics andSpectroscopy*, vol. 48, p. 1101, 1980.

[29] S.-K. Lee and I. Okura, "Optical sensor for oxygen using a porphyrin-doped sol-gel glass," *Analyst*, vol. 122, no. 1, pp. 81–84, 1997.

[30] S. Salhi, M. Vernières, C. Bied-Charreton, J. Faure, and A. Revillon, "New polymeric materials: porphyrins attached to preformed polystyrene," *New Journal of Chemistry*, vol. 18, no. 7, p. 783, 1994.

[31] D. A. Buttry and F. C. Anson, "New strategies for electrocatalysis at polymer-coated electrodes. Reduction of dioxygen by cobalt porphyrins immobilized in nafion coatings on graphite electrodes," *Journal of the American Chemical Society*, vol. 106, no. 1, pp. 59–64, 1984.

[32] J. E. Bennett and T. Malinski, "Conductive polymeric porphyrin films: application in the electrocatalytic oxidation of hydrazine," *Chemistry of Materials*, vol. 3, no. 3, pp. 490–495, 1991.

[33] X. Shi, K. M. Barkigia, J. Fajer, and C. M. Drain, "Design and synthesis of porphyrins bearing rigid hydrogen bonding motifs: highly versatile building blocks for self-assembly of polymers and discrete arrays," *Journal of Organic Chemistry*, vol. 66, no. 20, pp. 6513–6522, 2001.

[34] J. A. A. W. Elemans, R. van Hameren, R. J. M. Nolte, and A. E. Rowan, "Molecular materials by self-assembly of porphyrins, phthalocyanines, and perylenes," *Advanced Materials*, vol. 18, no. 10, pp. 1251–1266, 2006.

[35] F. de Loos, I. C. Reynhout, J. J. L. Cornelissen, A. E. Rowas, and R. J. M. Nolte, "Construction of functional porphyrin polystyrene nano-architectures by ATRP," *Chemical Communications*, vol. 1, pp. 60–62, 2005.

[36] P. A. J. De Witte, M. Castriciano, J. J. L. M. Cornelissen, L. M. Scolaro, R. J. M. Nolte, and A. E. Rowan, "Helical polymer-anchored porphyrin nanorods," *Chemistry—A European Journal*, vol. 9, no. 8, pp. 1775–1781, 2003.

[37] B. G. Choi, R. Song, W. Nam, and B. Jeong, "Iron porphyrins anchored to a thermosensitive polymeric core-shell nanosphere as a thermotropic catalyst," *Chemical Communications*, no. 23, pp. 2960–2962, 2005.

[38] J. Chen, P. Wagner, L. Tong, G. G. Wallace, D. L. Officer, and G. F. Swiegers, "A porphyrin-doped polymer catalyzes selective, light-assisted water oxidation in seawater," *Angewandte Chemie—International Edition*, vol. 51, no. 8, pp. 1907–1910, 2012.

[39] M. G. Walter, A. B. Rudine, and C. C. Wamser, "Porphyrins and phthalocyanines in solar photovoltaic cells," *Journal of Porphyrins and Phthalocyanines*, vol. 14, no. 9, pp. 759–792, 2010.

[40] N. Xiang, Y. Liu, W. Zhou et al., "Synthesis and characterization of porphyrin-terthiophene and oligothiophene $\pi$-conjugated copolymers for polymer solar cells," *European Polymer Journal*, vol. 46, no. 5, pp. 1084–1092, 2010.

[41] V. Cleave, G. Yahioglu, P. le Barny et al., "Transfer processes in semiconducting polymer-porphyrin blends," *Advanced Materials*, vol. 13, no. 1, pp. 44–47, 2001.

[42] H. Chen, J. Zeng, F. Deng, X. Luo, Z. Lei, and H. Li, "Synthesis and photophysical properties of porphyrin-containing polymers," *Journal of Polymer Research*, vol. 19, pp. 9880–9889, 2012.

[43] B. Li, X. Xu, M. Sun et al., "Porphyrin-cored star polymers as efficient nondoped red light-emitting materials," *Macromolecules*, vol. 39, no. 1, pp. 456–461, 2006.

[44] J. L. O'Donnell, N. Thaitrong, A. P. Nelson, and J. T. Hupp, "Liquid/liquid interface polymerized porphyrin membranes displaying size-selective molecular and ionic permeability," *Langmuir*, vol. 22, no. 4, pp. 1804–1809, 2006.

[45] C. Hsu, M. Nieh, and P. Lai, "Facile self-assembly of porphyrin-embedded polymeric vesicles for theranostic applicationsw," *Chemical Communications*, vol. 48, no. 75, pp. 9343–9345, 2012.

[46] C. Xing, Q. Xu, H. Tang, L. Liu, and S. Wang, "Conjugated polymer/porphyrin complexes for efficient energy transfer and improving light-activated antibacterial activity," *Journal of the American Chemical Society*, vol. 131, no. 36, pp. 13117–13124, 2009.

[47] A. Modak, M. Nandi, J. Mondal, and A. Bhaumik, "Porphyrin based porous organic polymers: novel synthetic strategy and exceptionally high $CO_2$ adsorption capacity," *Chemical Communications*, vol. 48, no. 2, pp. 248–250, 2012.

[48] T. Mathew and S. Kuriakose, "Cobalt(II) porphyrins supported on crosslinked polymer matrix as model compounds," *Journal of Porphyrins and Phthalocyanines*, vol. 3, no. 4, pp. 316–321, 1999.

[49] M. Schäferlinga and P. Bäuerle, "Porphyrin-functionalized oligo- and polythiophenes," *Journal of Materials Chemistry*, vol. 14, no. 7, pp. 1132–1141, 2004.

[50] A. D. Adler, F. R. Longo, J. D. Finarelli, J. Goldmacher, J. Assour, and L. Korsakoff, "A simplified synthesis for meso-tetraphenylporphin," *Journal of Organic Chemistry*, vol. 32, no. 2, p. 476, 1967.

[51] P. Rothemund, "Formation of porphyrins from pyrrole and aldehydes," *Journal of the American Chemical Society*, vol. 57, pp. 2010–2011, 1935.

[52] P. Rothemund, "A new porphyrin synthesis. The synthesis of porphin," *Journal of the American Chemical Society*, vol. 58, no. 4, pp. 625–627, 1936.

[53] G. D. Dorough, J. R. Miller, and F. M. Huennekens, "Spectra of the metallo-derivatives of $\alpha,\beta,\gamma,\delta$-tetraphenylporphine," *Journal of the American Chemical Society*, vol. 73, no. 9, pp. 4315–4320, 1951.

[54] A. Stone and E. B. Fleischer, "The molecular and crystal structure of porphyrin diacids," *Journal of the American Chemical Society*, vol. 90, no. 11, pp. 2735–2748, 1968.

[55] H. H. Chang, S.-Ch. Chen, D. Lin, and L. Cheng, "Preparation of bi-continuous Nylon-66 porous membranes by coagulation of incipient dopes in soft non-solvent baths," *Desalination*, vol. 313, pp. 77–86, 2013.

[56] M. Herrero, P. Benito, F. M. Labajos et al., "Structural characterization and thermal properties of polyamide 6.6/Mg, Al/adipate-LDH nanocomposites obtained by solid state polymerization," *Journal of Solid State Chemistry*, vol. 183, no. 7, pp. 1645–1651, 2010.

[57] D.-J. Lin, C.-L. Chang, C.-K. Lee, and L.-P. Cheng, "Fine structure and crystallinity of porous Nylon 66 membranes prepared by phase inversion in the water/formic acid/Nylon 66 system," *European Polymer Journal*, vol. 42, no. 2, pp. 356–367, 2006.

[58] H. W. Starkweather and R. E. Moynihan Jr., "Density, infrared absorption, and crystallinity in 66 and 610 nylons," *Journal of Polymer Science*, vol. 22, no. 102, pp. 363–368, 1956.

[59] A. M. Liquori, A. Mele, and V. Carelli, "Ultraviolet absorption spectra of polyamides," *Polymer Chemistry*, vol. 10, no. 5, pp. 510–512, 1953.

[60] M. A. García-Sánchez, S. R. Tello-Solís, R. Sosa-Fonseca, and A. Campero, "Fluorescent porphyrins trapped in monolithic $SiO_2$ gels," *Journal of Sol-Gel Science and Technology*, vol. 37, no. 2, pp. 93–97, 2006.

[61] M. A. García-Sánchez, V. de la Luz, M. L. Estrada-Rico et al., "Fluorescent porphyrins covalently bound to silica xerogel matrices," *Journal of Non-Crystalline Solids*, vol. 355, no. 2, pp. 120–125, 2009.

[62] M. A. García-Sánchez, V. de la Luz, M. I. Coahuila-Hernández, F. Rojas-González, S. R. Tello-Solís, and A. Campero, "Effects of the structure of entrapped substituted porphyrins on the textural characteristics of silica networks," *Journal of Photochemistry and Photobiology A*, vol. 223, no. 2-3, pp. 172–181, 2011.

[63] N. S. Allen, J. F. McKellar, and C. B. Chapman, "Formation of luminescent impurities during the polymerization of nylon 66," *Applied Polymer Science*, vol. 20, no. 6, pp. 1717–1719, 1976.

[64] N. S. Allen, J. F. McKellar, and G. O. Phillips, "Luminescence from thermally oxidized model amides in relation to nylon 66 degradation," *Journal of Polymer Science A*, vol. 12, no. 11, pp. 2623–2629, 1974.

[65] N. S. Allen, J. F. McKellar, and D. Wilson, "Quenching of chromophoric species in nylon-6,6 by halide ions," *Journal of Photochemistry*, vol. 6, no. 1, pp. 73–74, 1976-1977.

[66] N. S. Allen, J. F. McKellar, and D. Wilson, "Identification of the phosphorescent species in nylon 66," *Journal of Polymer Science A*, vol. 15, no. 11, pp. 2793–2795, 1977.

[67] Ch. M. Stellman, K. S. Booksh, and M. Myrick, "Multivariate fluorescence imaging of gel on nylon 66 production pack screens," *Applied Spectroscopy*, vol. 49, no. 11, pp. 1545–1549, 1995.

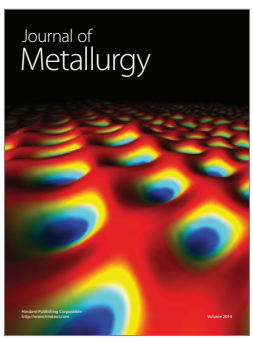

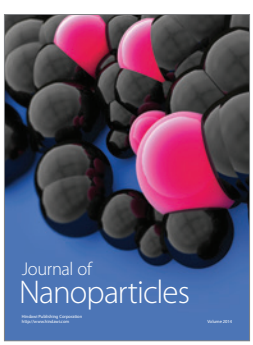

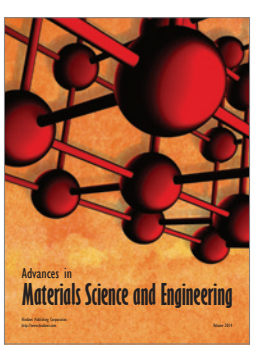

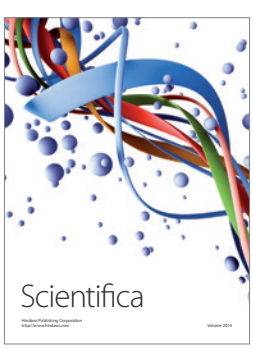

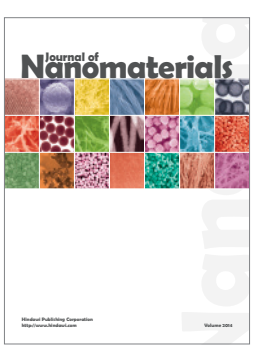

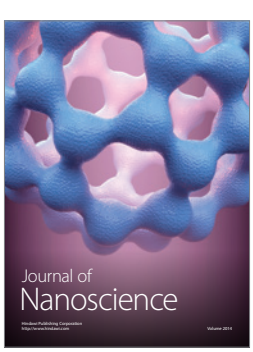

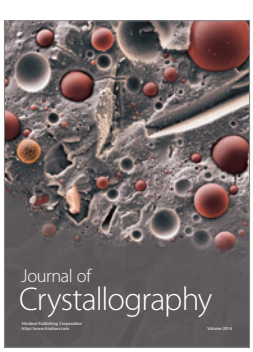

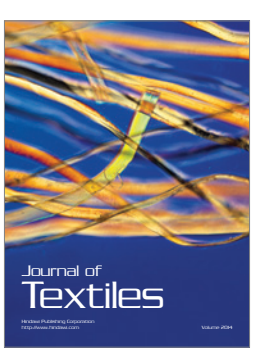


Hindawi

Submit your manuscripts at
http://www.hindawi.com